Sensors and Actuators B 204 (2014) 224–230

Contents lists available at ScienceDirect

Sensors and Actuators B: Chemical

journal homepage: www.elsevier.com/locate/snb

Hierarchical flower-like WO_3 nanostructures and their gas sensing properties

Chong Wang, Ruize Sun, Xin Li, Yanfeng Sun*, Peng Sun, Fengmin Liu, Geyu Lu*

State Key Laboratory on Integrated Optoelectronics, College of Electronic Science and Engineering, Jilin University, 2699 Qianjin Street, Changchun 130012, People's Republic of China

ARTICLE INFO

Article history:
Received 18 May 2014
Received in revised form 16 July 2014
Accepted 17 July 2014
Available online 27 July 2014

Keywords:
WO_3
Hierarchical nanostructure
Flower-like
NO_2 sensor

ABSTRACT

Flower-like WO_3 composed of nanosheets were successfully synthesized by calcining the acid-treated hydrothermal precursor. Field emission scanning electron microscopy and transmission electron microscopy results reveal that the flower-like WO_3 are assembled by a number of irregular-shaped nanosheets, which are cross-linked in the interior of the microflower. A possible formation mechanism is proposed on the basis of the results of time-dependent experiments. Moreover, the gas sensing properties of the obtained flower-like nanostructured WO_3 were investigated. It is found that the sensor based on the flower-like WO_3 nanostructure exhibits good selectivity and high response to NO_2, and the detection limit is about 2 ppb.

1. Introduction

In recent years, functional materials have been extensively studied due to their unique physical and chemical properties compared to solid structures [1]. Among them, oxide semiconductor materials occupy an important position. Therefore, much effort has been devoted to the study of various oxide semiconductor materials such as ZnO [2,3], SnO_2 [4,5], CuO [6,7], In_2O_3 [8,9] and TiO_2 [10,11].

Tungsten oxide is a very important n-type ($Eg \approx 3.2$ eV) oxide semiconductor which offers manifold technological applications including lithium ion batteries, photoelectrochemical, solar energy and so on [12–15]. One of the most important applications of WO_3 material is in gas sensors which has been found to show remarkable gas sensing properties for the detection of NO_2 [38–40]. Due to its excellent performance and practical application, a variety of routes have been employed to obtain WO_3 crystal such as thermal evaporation [16], electrochemical precipitation [17] and sol–gel [18]. It is well known that high response and superior selectivity are important parameters in designing semiconductor gas sensors [19]. Therefore, increasing the response and improving the selectivity of oxide semiconductor gas sensors are major scientific challenges for developing new sensor strategies. As many groups have reported before, the morphology plays an important role in determining the properties of materials [20–22]. Hence, various morphologies of WO_3 with different dimensional nanostructures have been synthesized in order to improve the performance of devices based on WO_3, such as nanowire [23], nanoplate [24], hollow-sphere [25], urchin-like [26] and many other hierarchically complex micro/nanostructures [27–30]. However, it is still a challenge to organize the 1D/2D WO_3 nanostructure into well-defined 3D nanostructure in order to obtain high performance NO_2 gas sensor.

In this work, the precursor was synthesized by using $NiCl_2{\cdot}6H_2O$ and $Na_2WO_4{\cdot}2H_2O$ through a hydrothermal method. Then, an acid-treated method and subsequent heat treatment at 500 °C for 2 h were used to prepare the flower-like WO_3. Moreover, the formation process has been investigated through the morphology evolution with different acidification times, and a possible formation mechanism is speculated. The sensors based on the synthesized flower-like WO_3 exhibit a high response to NO_2, and the response of the sensor to 2 ppb NO_2 is about 12.8. To our knowledge, WO_3 with this novel nanostructure with such high sensitivity was first synthesized.

2. Experimental

All the reagents (analytical-grade purity) were used without any further purification.

The precursor was synthesized under hydrothermal condition. In a typical synthesis, 4 mmol $Na_2WO_4{\cdot}2H_2O$ and 0.8 g of sodium dodecyl benzene sulfonate (SDBS) were dissolved in 20 ml distilled water to form a homogeneous solution under vigorous stirring.

* Corresponding authors. Fax: +86 431 85167808.
E-mail addresses: syf@jlu.edu.cn (Y. Sun), lugy@jlu.edu.cn (G. Lu).

http://dx.doi.org/10.1016/j.snb.2014.07.083
0925-4005/

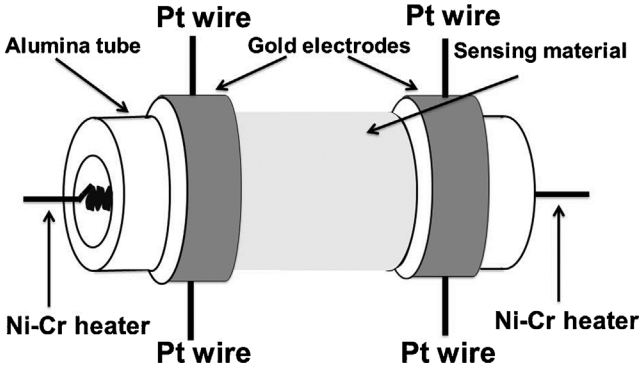

Fig. 1. Schematic structure of the gas sensor.

Then 20 ml aqueous $NiCl_2$ solution (0.2 M) was added into the above solution. Ten minutes later, the mixture solution was transferred into a Teflon-lined stainless steel autoclave, sealed tightly, and maintained at 160 °C for 24 h. After the autoclave was cooled to room temperature naturally, the green product was collected by washing with deionized water and absolute ethanol for several times, and dried at 80 °C for 1 day.

To get the flower-like WO_3 sample, the acidification experiment was then performed. The green precursor was immersed in 4 M HNO_3 and maintained at room temperature for 21 h statically. During this process, the color of the solution was changed gradually from green to yellow. The yellow product was then washed with deionized water and absolute ethanol for several times and dried at 80 °C in air. Finally, the acid-treated product was calcined at 500 °C to get the WO_3 sample.

A sensor device was fabricated using the obtained WO_3 powder. Firstly, a suitable amount of WO_3 powder was mixed with ethanol to obtain a paste which was then coated onto an alumina tube (4 mm in length, 1.2 mm in external diameter and 0.8 mm in internal diameter) using a small brush slowly and lightly. The tube was installed with a pair of gold electrodes, and each electrode was connected with two Pt wires. After drying in air for a while, the thin film with proper thickness was formed. Then the tube was placed in a muffle furnace and the temperature was kept at 300 °C for 2 h. When the temperature was reduced to room temperature, the tube with sensing film was soldered to the pedestal. Finally, a Ni–Cr alloy coil was inserted into the alumina tube as a heater in order to control the operating temperature of the sensor. The structure of the sensor is shown in Fig. 1. The gas-sensing properties of the sensor were measured with a static gas-sensing characterization system, as diagrammed in Fig. 2: sensor was put to the testing chamber from the air chamber, standard NO_2 gas with a certain concentration was injected into the testing chamber in order to get NO_2 gas with ideal concentration. When the resistance reached Rg, the gas is discharged with the help of air intake and exhaust system and electrical fan. The response of the sensor is defined as $S = Rg/Ra$ for oxidizing gas or Ra/Rg for reducing gas, here, Ra and Rg are the resistances of the sensor in the air and target gas, respectively. The response time and recovery time are defined as the time taken by the sensor to achieve 90% of the total resistance change during the adsorption and desorption process, respectively.

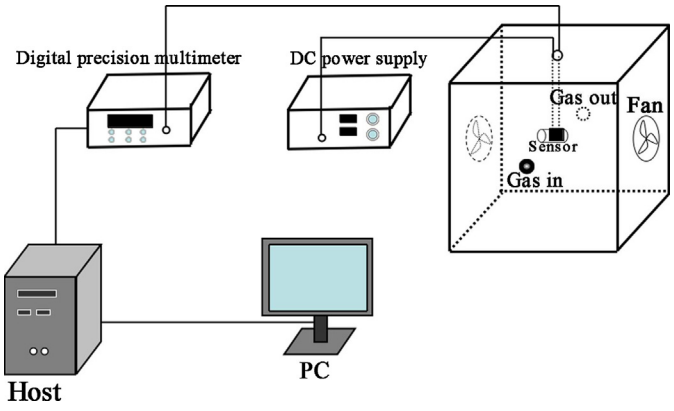

Fig. 2. Testing schematic diagram.

The crystal phase and morphologies of the acid-treated products and calcined products were observed by X-ray powder diffraction (XRD, Rigaku D/max-2550) with Cu Kα1 radiation (λ = 0.15406 nm) at 50 kV/200 mA and the scanning speed was 12° per minute, field emission scanning electron microscopy (SEM, JEOL JSM-7500F, 15 kV), high resolution transmission electron microscopy (HRTEM, JEM 2100F, 200 kV), and selected area electron diffraction (SAED). Thermogravimetric (TG) analysis and differential scanning calorimetric (DSC) measurements were also carried out using a NETZSCH STA 449F3 simultaneous thermogravimetric analyzer under air atmosphere in the temperature range from 25 to 800 °C with a heating rate of 10 °C min^{-1}.

3. Results and discussion

3.1. Structural and morphological characteristics of the prepared WO_3

The XRD patterns of the precursor are given in Fig. S1. The diffraction peaks could not be well indexed to a known substance (not shown here). Fig. 3 shows the XRD patterns of acid-treated product and the sample obtained by calcining acid-treated product at 500 °C. It can be seen that before calcination (Fig. 3b), all the diffraction peaks could be indexed to $H_2W_4O_{13}$ (JCPDS file no.1-583). No peaks of other impurity phases are detected from this pattern. And after calcining at 500 °C, $H_2W_4O_{13}$ was converted into pure monoclinic structure of WO_3 according to JCPDS card No. 89-4480. No characteristic peaks from any other impurities can be observed, indicating that no impurity exists and the $H_2W_4O_{13}$ has completely transformed into the monoclinic WO_3 phase after calcining.

The morphologies and microstructures of the acid-treated and calcined products were illustrated by FESEM observations. Fig. 4a and b shows the detailed morphology of the acid-treated sample, from which 3D flower-like nanostructures with fine nanosheet building units are clearly observed. The average diameter of the

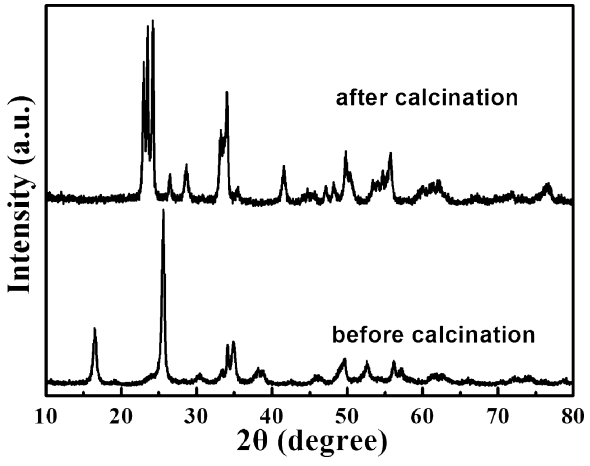

Fig. 3. X-ray diffraction patterns of the as-prepared samples before and after calcining.